

A similarity approach to turbulent sediment-laden flows in open channels

By D. A. LYN

Institute for Hydromechanics, University of Karlsruhe, D-7500 Karlsruhe 1, West Germany

(Received 2 January 1987 and in revised form 13 November 1987)

A basis is developed for a similarity treatment of the coupled mean fields in turbulent open-channel flows over a flat sand bed in equilibrium with a suspension of sand. Hypotheses involving multiple scales, asymptotic similarity, and matching over an overlapping region are made instead of the traditional dependence on eddy diffusion and Reynolds analogies. Velocity measurements using the laser-Doppler technique in experiments with well-sorted natural sands showed that, contrary to the implications of previous models, the effect of suspended sediment on the mean velocity profile may, over a variety of laboratory conditions, be confined to a layer adjacent to the bed. This is interpreted within the similarity framework in terms of the existence of an inner lengthscale, differing from either the viscous or the grain scale, associated with the presence of sediment. The suggested lengthscales and concentration scales are examined in light of the experimental results.

1. Introduction

Turbulent sediment-laden flows in open channels are of direct concern to river engineers and geomorphologists, but are also relevant in the analysis of related problems such as coastal sediment transport and transport of solids in pipelines. Such flows should interest researchers of wall turbulence in general because the presence of sediment may loosely be considered as a perturbation of an homogeneous-fluid flow, the investigation of which may shed light on flows without sediment. The problem is, in general, a coupled one in that the sediment can no longer be considered a passive contaminant and, in this, resembles problems with buoyancy effects. This analogy with stably stratified flows has been more broadly applied to sediment-laden flows, and its range of validity is one of the questions with which the present work is concerned. The discussion is limited to the simple case of a flow uniform in the streamwise direction over a flat bed (a definition sketch is given in figure 1), inclined at a slope, S , of depth, h . Flow over bed forms, such as dunes or ripples, is not considered; attention is restricted to the effect of the presence of sediment on wall turbulence. The particles, i.e. sand grains, are assumed uniform in size and relative density, s , with a diameter, d , where non-hydrodynamic effects are negligible. In the bulk of the flow, the suspension is typically dilute, the volume concentration being of $O(10^{-3})$ or less. Only the mean velocity and concentration profiles are considered; a subsequent paper will deal with higher-order statistics.

Similarity or scaling ideas have been little exploited in the analysis of sediment-laden flows mainly because of the dominance of the mixing-length or eddy-diffusivity models. Moreover, in sediment-laden flows, appropriate scales are not clear, or are thought to be too many to yield any simplification. Nevertheless, the similarity approach can provide a consistent framework, although perhaps not the only one,

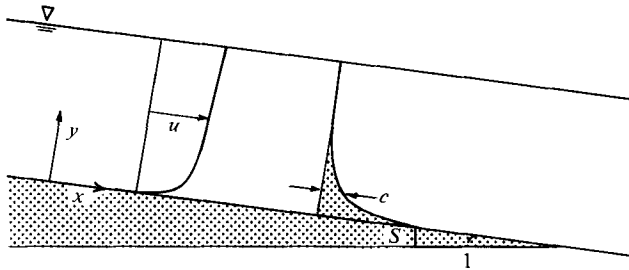


FIGURE 1. Definition sketch.

within which both the mean velocity and concentration fields can be treated in parallel as befits a coupled problem. It avoids detailed dynamic considerations, about which very little is known, thereby avoiding perhaps overly simplified models. This is balanced however by the need for additional empiricism. The formal approach is outlined in §3, where the appropriate lengthscales and concentration scales are discussed.

Experiments were performed to examine the validity of previous models, particularly those based on the analogy to stably stratified shear flows, as well as to develop an empirical basis for a similarity theory. The mean velocity profile receives primary attention since this has been more intensively studied in the past and some controversy has arisen about it. A two-component laser-Doppler velocimetry (LDV) system was used to measure local mean stress (= Reynolds stress), as well as the local mean velocity. Unlike some well-known experiments (e.g. Vanoni 1946; Coleman 1981), attention is focused on sediment-laden flows in equilibrium with a sand bed, here termed equilibrium-bed flows. These are conceptually, if perhaps not experimentally, simpler to treat than sediment-laden flows in the absence of a sand bed, here termed starved-bed flows. Nevertheless, the latter were also investigated as a complement to the study of equilibrium-bed flows. Preliminary experiments with clear-water (no suspension) flows provided a precise basis of comparison since experimental conditions including instrumentation were comparable or identical. Although the main experimental attention is given to the velocity profile, detailed vertical profiles of local mean concentrations were also obtained, in keeping with the emphasis on the coupled nature of the problem. For these, the conventional suction sampling technique was used. Experimental details are discussed in §4, and results are presented and discussed in §5.

2. A critical review of previous approaches

2.1. Velocity-defect profiles

In the hydraulics of open-channel flow without sediment, the velocity-defect profile is usually described by a logarithmic function throughout the depth; i.e.

$$\frac{\bar{u} - \bar{u}_{\max}}{u_*} = \frac{1}{\kappa} \ln \frac{y}{h}, \quad (2.1)$$

where the von Kármán constant, $\kappa \approx 0.4$, and \bar{u}_{\max} is the maximum velocity attained in the flow, assumed to occur at the free surface, $y = h$. Vanoni (1946) fitted a profile like (2.1) to velocity profiles in starved-bed flows, but found that a variable $\kappa_s < \kappa$

was necessary in order to obtain any reasonable agreement. This apparent reduction in κ was attributed to a damping of turbulence by the suspended sediment (see also Saffman 1962). As the basis of a purely empirical fitting procedure, (2.1) might be useful if reliable predictions of κ_s could be made; the most well-known correlation for κ_s (Einstein & Chien 1955) exhibits, however, a large scatter. The traditional approach may be said to view the effect of sediment as being of a global nature, since the reduced κ affects the shape of the entire velocity profile. The validity of (2.1) has recently been challenged (Itakura & Kishi 1980; Coleman 1981) by models based on a simple analogy between sediment-laden flows and weakly stable stratified flows. The possible importance of buoyancy effects or effects analogous to buoyancy had been previously suggested by several workers: Barton & Lin (1955) and Hino (1963) in the specific context of flows in alluvial streams, and Barenblatt (1953, 1979), Batchelor (1965), Monin & Yaglom (1971) and Lumley (1976) in the context of particulate flows in general. It is notable that while early work on the stratified atmosphere also made use of a variable κ (Sheppard 1946), this has been completely superseded by the Monin–Oboukhov theory (Monin & Yaglom 1971), in which κ remains constant.

Itakura & Kishi (1980) adapted the formalism of the Monin–Oboukhov similarity theory (see also Monin & Yaglom 1971; Lumley 1976) to sediment-laden flows in open channels and proposed $L_s \equiv u_*^3/w_s g(s-1) \langle \bar{c} \rangle$ as a Monin–Oboukhov length-scale, where $\langle \bar{c} \rangle$ is the depth-averaged concentration, w_s a characteristic settling velocity of a particle in a turbulent suspension, g the gravitational constant. They argued therefore that, instead of a pure log law as in (2.1), the log-linear law, characteristic of the Monin–Oboukhov theory of weakly stable stratified flows, should give a better description of the velocity-defect profile. This adaptation faces several criticisms. In its clearest form, the original theory assumes constant fluxes of momentum and buoyancy which allow the definition of a unique lengthscale. Further, these fluxes are determined by boundary values. Fluxes in sediment-laden open-channel flows vary, and, in the case of the local settling flux, this variation may be substantial, particularly near the bed. Moreover, although the momentum flux at the boundary may be known, nothing is known of the concentration, and hence of the buoyancy flux, at the boundary.

The Monin–Oboukhov approach retains the universal constancy of κ and incorporates the effect of sediment through a linear correction function, depending on a type of Richardson number; except that the correction function is no longer linear, the profile suggested by Coleman (1981),

$$\frac{\bar{u} - \bar{u}_{\max}}{u_*} = \frac{1}{\kappa} \ln \frac{y}{y_{\max}} - \frac{2W_0}{\kappa} \cos^2 \left(\frac{1}{2}\pi \frac{y}{y_{\max}} \right), \quad (2.2)$$

is conceptually identical. The correction function is adapted from the universal profile used by Coles (1971) to describe general boundary-layer flows, where y_{\max} is defined by the relation, $\bar{u}(y_{\max}) \equiv \bar{u}_{\max}$. The so-called wake coefficient, W_0 (≈ 0.2 in clear-water flows), is allowed to vary in sediment-laden flow, and Coleman correlated it with what was termed a bulk Richardson number, which in the present context may be taken to be $Ri_C = g(s-1) c_0 y_{\max} / u_*^2$, c_0 being the concentration at $y = 0$, thus implicitly defining a lengthscale, $L_C = u_*^2 / g(s-1) c_0$. From starved-bed experiments, Coleman estimated that Ri_C may attain magnitudes up to 200. Interpreted in terms of the analogy to stably stratified flows, large magnitudes of Ri_C imply extremely stable flows in which turbulence should be practically extinguished. This is evidently

not the case as turbulence must remain important in order to sustain the suspension. The models based on the analogy to stably stratified flows imply that the effect of sediment should be observable primarily in the outer flow, the inner flow being still dominated by boundary shear and viscosity. This contrasts with the traditional view which favour a more global effect. Nevertheless, both types of models agree qualitatively to some extent since both suggest an inhibition of vertical transport, (the reduced κ_s being equivalent to a reduced mixing length), and the Einstein–Chien correlation for κ_s involves a parameter very similar to h/L_s .

2.2. The concentration profile

The concentration profile has invariably been derived from an equation representing the balance between the upward turbulent flux of sediment and the downward flux due to gravitational settling. Often the former is taken to be $-\overline{c'v'}$, while the latter is $w_s \bar{c}$, such that

$$-\overline{c'v'} + w_s \bar{c} = 0. \quad (2.3)$$

An eddy-diffusivity model for $-\overline{c'v'}$ is then invoked. For example, the traditional choice based on Reynolds analogy leads to the profile

$$\frac{\bar{c}}{c_a} = \left(\frac{a/h}{1-a/h} \frac{1-y/h}{y/h} \right)^{Z_R}, \quad (2.4)$$

where the Rouse exponent, $Z_R \equiv w_s/\beta_s \kappa_s u_* \beta_s$ is a proportionality constant, and c_a is a reference concentration at an arbitrary reference elevation, $y = a$. Because κ_s and β_s have yet to be reliably correlated, the sensitivity of (2.4) to the value of Z_R reduces its predictive value. A further complication in the use of (2.3) regards the appropriate value for w_s , which is likely to differ from the settling velocity of an isolated particle in a stagnant fluid. Even as the basis of an empirical fit, with Z_R as an adjustable parameter, it has been recognized that (2.4) does not adequately agree with experimental results. Suggestions for improvements have usually proposed different eddy diffusivities for different flow regions (Batchelor 1965; van Rijn 1984).

3. Similarity and sediment-laden flows

3.1. Motivation

Since the well-known matching argument (Izakovson 1937; Millikan 1939) applies to the velocity profile in uniform open-channel flows without sediment, an analogous treatment of sediment-laden flows may be motivated as an alternative to traditional mixing-length or eddy-diffusivity concepts. Such an approach should treat both the velocity and the concentration profiles in parallel. If the standard argument is applied without modification to the concentration profile, then the formal similarity hypotheses, the inner and outer laws, are formulated as

$$\left(\frac{c}{c_*} \right)_i = f \left(\frac{y}{l_i} \right), \quad (3.1)$$

$$\left(\frac{c}{c_*} \right)_o = F \left(\frac{y}{l_o} \right), \quad (3.2)$$

where c_* is an appropriate concentration scale (e.g. the boundary concentration, in analogy to the shear velocity, u_*), l_i and l_o are inner and outer length scales

(e.g. $l_i = l_v \equiv \nu/u_*$, the viscous scale, and $l_o = h$), f and F are asymptotic functions describing the profile in the corresponding regions, and the subscripts i and o indicate inner and outer variables. From these hypotheses, and the assumption of the existence of an overlap region where both asymptotic descriptions are simultaneously valid, it must be concluded that, like the velocity profile, the concentration profile also follows a log law in the overlap region. This reasoning is appropriate for the temperature profile in the Monin–Oboukhov theory of the weakly stable atmospheric surface layer. A log law does not, however, describe the concentration profile in sediment-laden flows. A qualitative difference between the coupled mean fields is found which has no equivalent in stratified flows of Monin–Oboukhov type, again an indication perhaps of the inadequacy of any simple and generally applicable analogy between the two problems.

In the Appendix, it is shown that log law is a special case, which applies when a single scale for the dependent variable, whether u_* or c_* , is common to both inner and outer regions. More generally, power laws can be obtained by matching arguments, but these require disparate scales not only for the independent but also for the dependent variable. Whether power laws are the most general functional forms derivable from this type of matching argument is not clear; it suffices here that they represent a wider class of functions, more useful in describing concentration profiles. Therefore, it shall be hypothesized that the concentration field in open-channel sediment-laden flows is characterized by two disparate concentration scales, to be denoted by c_s and c_h , for the inner and outer regions respectively. This contrasts with the implicit assumptions of previous work, where only a single scale such as the depth-averaged concentration (Itakura & Kishi 1980; Einstein & Chien 1955), or the boundary concentration (Coleman 1981), is mentioned. The previously noted hybrid character of Ri_c , which resulted in inconsistently large values, might, in light of this discussion, be corrected by using a length appropriate to the inner region instead of h , or a concentration scale appropriate to the outer region instead of the boundary concentration, c_o .

In the standard treatment of pipe or channel flow without sediment, the von Kármán constant, κ , arises as a matching constant independent of the Reynolds number, the only dimensionless parameter in the simple problem. For sediment-laden flows, where additional dimensionless parameters are relevant, the traditional model may be interpreted as arguing that κ_s may well vary. The matching argument does not preclude such a possibility; it places, however, a restriction on the choice of such a parameter, with which κ_s may vary. Since κ_s is involved in asymptotic expressions for both inner and outer laws, it can only vary with a parameter which is independent of any purely local scales. This implies that the Einstein–Chien parameter, which is roughly equivalent to h/L_s , is inconsistent in this regard, since h , at least, is a purely local lengthscale, being irrelevant in the inner region. One consistent choice might be w_s/u_* , since neither velocity is purely local (this assumes that u_* continues to be appropriate for both inner and outer regions). The theory of Barenblatt (1979) indeed predicts such a variation, and is thus at least consistent. In contrast to the special case of the log law, which is associated with a single matching constant, the more general power law is associated with two matching constants, a multiplicative constant like κ , as well as the exponent in the power law. The general possibility of a variation of both of these constant must also be acknowledged, again with the provision that the dimensionless parameter with which they vary involves no purely local parameter. The exponent may then vary in a general way such as not to be deducible from purely dimensional arguments (see Barenblatt 1979). A power

law with an exponent varying with a dimensionless parameter may be particularly relevant to the description of the concentration profile since the traditional result (2.4) reduces to such a law in the asymptotic case when $y/h \ll 1$.

3.2. Similarity hypotheses

A similarity approach to the description of sediment-laden flows in open-channels is proposed based on the following hypotheses:

- (i) There exists a region of flow in which only two lengthscales: an inner lengthscale, l_s , and an outer length, h (the depth of flow), are important.
- (ii) For the velocity profile,
 - (a) a single common velocity scale, u_* (the shear velocity), characterizes both inner and outer regions, and
 - (b) no dimensionless parameter is relevant in the outer region.
- (iii) For the concentration profile,
 - (a) two disparate concentration scales, c_s and c_h , exist, and
 - (b) a dimensionless parameter, β , is important in both inner and outer regions.
- (iv) In each region, asymptotic similarity in the inner or the outer variable, as the case may be, prevails.

In mathematical form, these hypotheses may be stated in terms of inner similarity laws:

$$\frac{\bar{u}}{u_*} = f(\xi_s; \alpha_1), \quad (3.3)$$

$$\frac{\bar{c}}{c_s} = g(\xi_s; \beta), \quad (3.4)$$

and of outer similarity laws:

$$\frac{\bar{u} - \bar{u}_{\max}}{u_*} = F(\varphi) \quad (3.5)$$

$$\frac{\bar{c}}{c_h} = G(\varphi; \beta), \quad (3.6)$$

where $\xi_s = y/l_s$, $\varphi = y/h$ and α_1 and β are dimensionless parameters, the former important only in the inner region, the latter important in both inner and outer regions.

The common velocity scale excludes a power-law velocity profile, and implies a logarithmic profile in the overlap layer. The hypothesis (ii**b**) implies further that the von Kármán constant remains the same as in clear-water flows, i.e. $\kappa_s = \kappa \approx 0.4$, and also that the outer-flow component is unaffected by the presence of suspended sediment. The effect of sediment is characterized by an inner lengthscale, l_s , distinct from the inner lengthscales of importance in clear-water flows. The inclusion of the parameter, α_1 , allows an additive constant in the log law (expressed in inner coordinates) which may depend on factors such as roughness (in which case α_1 might be a roughness Reynolds number). Disparate concentration scales permit power-law concentration profiles, in contrast to the velocity profile, while a dimensionless parameter, β , important in both inner and outer regions, permits a varying exponent. Asymptotic log and power laws may be found only if $l_s \ll h$. The possibility that the effects of sediment may extend throughout the flow, such that $l_s \sim h$ is not ruled out. In such cases, the asymptotic results cannot be justified without additional assumptions. Although the viscous scale, l_v , and the characteristic sand size, d , are

assumed unimportant in the region under consideration, they may be essential in other regions of the flow, e.g. very near the bed. The similarity approach is therefore most useful if a region exists where l_v (or d) $\ll l_s \ll h$. Coupling between the velocity and concentration fields is achieved, not through an appeal to a Reynolds analogy, but through the assumption that the same lengthscales, l_s and h , are important for determining the coupled fields.

3.3. An inner lengthscale for sediment-laden flows

A general dimensional relation between l_s and the other physical parameters assumed to be relevant in the inner region may be expressed as

$$\mathcal{F}_l(l_s, u_*, d, g(s-1), w_{s0}) = 0, \quad (3.7)$$

where w_{s0} is the settling velocity of an isolated characteristic particle in a stagnant fluid. This should be conceptually distinguished from w_s , used in previous approaches, which is the settling velocity of a particle in a sediment-laden turbulent flow. The choice of 'basis' parameters is somewhat arbitrary, since ν could have been included instead of w_{s0} , because a standard drag curve relates $g(s-1)$, d , ν and w_{s0} . The particular choice made in (3.7) is motivated by the use of w_s in previous treatments of the concentration profile, and so facilitates comparison with the traditional result. Unlike w_s , w_{s0} unambiguously characterizes the grain and the fluid and is independent of the particular flow. It follows that

$$\Delta_s \equiv \frac{g(s-1)l_s}{u_*^2} = \mathcal{E}\left(\frac{w_{s0}}{u_*}, \frac{g(s-1)d}{w_{s0}^2}\right). \quad (3.8)$$

Thus, for given grain characteristics, d , s , and w_{s0} , the non-dimensional inner lengthscale, Δ_s , depends solely on the ratio, w_{s0}/u_* .

It may be hoped that (3.8) simplifies in asymptotic cases. As w_{s0}/u_* becomes large, there will no longer be any sediment in suspension and so no effect will be observed in the velocity profile. This suggests that, in this case, $l_s \rightarrow 0$, and other lengthscales, such as l_v or d , regain their importance. At the other extreme, the case where $w_{s0}/u_* \rightarrow 0$ is complicated by questions of saturation (is the suspension in equilibrium with the bed?) and of possible changes in the nature of the flow (are non-Newtonian effects important?). The intermediate case, in which w_{s0}/u_* remains finite but $l_s \gg d$ (or l_v) is of some interest. It is hypothesized that, in this case, d ceases to be a relevant parameter in the region, $y/l_s \geq O(1)$. This hypothesis yields

$$\Delta_s = \mathcal{E}_\infty\left(\frac{w_{s0}}{u_*}\right), \quad (3.9)$$

$$l_s = \frac{u_*^2}{g(s-1)} \mathcal{E}_\infty\left(\frac{w_{s0}}{u_*}\right). \quad (3.10)$$

The difficulty and the distinction from other better known flows lie in that l_s is here defined in terms of an unknown function, \mathcal{E} (or \mathcal{E}_∞), which must be determined from experiments. This determination presumes however an operational definition of l_s , such as the point at which the velocity-defect profile begins to deviate from the velocity-defect profile for clear-water experiments, which necessarily suffers from some imprecision and arbitrariness.

3.4. Concentration scales

The proposed similarity theory hypothesizes the existence of two disparate concentration scales. Consider therefore a general dimensional relation between the outer concentration scale, c_h , and the other relevant parameters,

$$\mathcal{F}_c(c_h, u_\star; h, g(s-1), w_{s0}) = 0. \quad (3.11)$$

Note that c_h is considered as distinct from $g(s-1)$; the essence of the stratified-flow analogy lies in the assumption that $g(s-1)$ and c_h must be considered together as a single group, $g(s-1)c_h$. The more general formulation of (3.11) includes the possibility that the suspension has an effect depending on the concentration beyond that of buoyancy. The increased generality is however purchased at the cost of not being able to rely on dimensional reasoning alone, which can only give

$$\Pi_h\left(\frac{g(s-1)h}{u_\star^2}, c_h, \frac{w_{s0}}{u_\star}\right) = 0. \quad (3.12)$$

To obtain any simplification, a further hypothesis must be made. This may be, at least formally, motivated from the stratified-flow analogy and leads to the outer scale,

$$c_h = \left(\frac{u_\star^2}{g(s-1)h} \mathcal{E}_h\left(\frac{w_{s0}}{u_\star}\right)\right)^Z, \quad (3.13)$$

and to the inner scale,

$$c_s = \left(\frac{u_\star^2}{g(s-1)l_s} \mathcal{E}_s\left(\frac{w_{s0}}{u_\star}\right)\right)^Z, \quad (3.14)$$

where \mathcal{E}_h and \mathcal{E}_s are expected to be $O(1)$, and the exponent, Z , can only depend on a dimensionless parameter, β , important in both regions of the flow. In the stratified-flow analogy, Z would be unity, as can be deduced from dimensional considerations.

The choice of (3.13) and (3.14) as inner and outer concentration scales implies a power law with a variable exponent, $-Z$, in the overlap region. The stratified-flow analogy predicts therefore that $c \sim y^{-1}$ (see Barenblatt 1979). In (3.13–3.14), w_{s0}/u_\star is the only dimensionless parameter assumed to be relevant in both inner and outer regions. It follows then that the exponent, Z , as well as any multiplicative and additive constants arising from the matching, are functions of this parameter only; i.e.

$$Z = Z(\beta) = Z\left(\frac{w_{s0}}{u_\star}\right). \quad (3.15)$$

This leads to a particularly simple expression for the asymptotic law in the overlapping region,

$$c \approx \left(\frac{u_\star^2}{g(s-1)y} \mathcal{E}\left(\frac{w_{s0}}{u_\star}\right)\right)^Z, \quad (3.16)$$

where any multiplicative constant has been absorbed in the function, $\mathcal{E}(w_{s0}/u_\star)$, and an additive constant of zero has been assumed for simplicity. The simple asymptotic form for l_s (3.10) is also seen to lead to a correspondingly simple asymptotic form for c_s , namely,

$$c_s = c_{s\infty} \left(\frac{w_{s0}}{u_\star}\right). \quad (3.17)$$

4. Experimental considerations

4.1. Experimental apparatus

Experiments were performed in a 13 m long, 26.7 cm wide, tiltable recirculating flume, and observations were taken at a section, ≈ 9 m from the channel entrance. The bare flume is not smooth, being covered by an epoxied layer of fine sand, estimated to be of diameter, 0.15 mm or less. The flume sidewalls had no such layer, although some roughness stemmed from uneven paint. The suction sampler, used for measuring local concentration, was a 6.3 mm o.d. brass tube, bent at right-angles, with a tip flattened to give an approximately rectangular opening, 1 mm high and 5.6 mm wide. The LDV system, operated in the real-fringe mode, is a three-beam single-colour system, with a 200 mW argon-ion laser as light source. It is distinguished by rather large intersection angles ($\approx 20^\circ$ in air), used to obtain a compact probe volume, thus reducing noise from extraneous scattering by sand grains. The resulting probe volume was ≈ 2 mm long and ≈ 0.3 mm wide, with a fringe spacing of ≈ 1 μm . Measurements were made only on the centreline of the flume. The three-beam configuration was chosen in order to allow measurements closer to the bottom without compromising on the large intersection angles, but, by the same token, two-component measurements were not possible close to the free surface. In the context of mean profiles, the two-component measurements were used in the estimation of the wall shear (and hence u_*) from the extrapolation of the measured Reynolds stress profile to the boundary. The importance of an estimate of wall shear independent of the velocity profile is seen in that the common estimate of u_* assuming a log law and that $\kappa = 0.4$ is questionable, since both the log law and the value of κ_s are in doubt in sediment-laden flows. In preliminary experiments with clear-water, where the conventional assumptions are justified, estimates of u_* from the velocity profile and the stress profile were in good agreement (Lyn 1986). In the case of an equilibrium bed, the definition of a lower boundary is somewhat problematic; here the conventional definition as the point at which the bed is found after the cessation of flow is used. The mean-velocity results to be presented were obtained from one-component measurements, since these were obtained throughout the depth.

The presence of two types of scattering particles, tracers and sand grains, pose the problem of distinguishing between the two. The large disparity in size (tracer particle < 10 μm , sand grain > 150 μm) provides one possible means of distinction since this should lead to large differences in the pedestal of the Doppler signal. Pedestals were therefore sorted into five size classes, but a sharp separation between the two types of scatterers could not be obtained on this basis. Nevertheless, the sorting scheme was retained, and only the smallest size class was used in the determination of the fluid velocity, this with the aim of minimizing the contamination of tracer-particle data by sand-grain data. This identification problem is expected to be alleviated by the diluteness of the suspension where measurements could be taken, such that the great majority of velocity realizations are likely to be those initiated by tracer particles. Computed statistics of fluid velocity should not therefore be especially sensitive to relatively rare errors in identification.

The problem of statistical bias due to the nature of the LDV sampling was ignored in this study for several reasons. In open-channel flows, this bias is comparatively unimportant in the bulk of the measurement region because the relative intensity, $(\overline{u'^2})^{1/2}/\bar{u}$, is small ($< 15\%$). Further, the effect of the presence of sediment on this bias is uncertain, and may even produce a compensating bias. Finally, being a

Symbol	Equilibrium-bed				Starved-bed					
					1957ST-1		1957ST-2			
	1565 EQ	1965 EQ	2565 EQ	1957 EQ	A ◇	B ○	A ✱	B ⊕	C ⊕	D ◁
Temperature, T (°C)	20.7	21.1	21.3	20.9	21.1	21.4	21.2	21.1	21.6	21.3
Discharge	10.8	11.1	12.1	9.9	10.3	10.3	12.1	12.4	12.6	12.6
Depth, h (cm)	6.45	6.51	6.54	5.72	5.69	5.68	5.84	5.77	5.75	5.74
Slope, S ($\times 10^{-3}$)	2.44	2.51	2.96	2.95	2.99	2.98	4.00	3.95	4.00	4.00
u_*^a (cm/s)	3.58	3.75	4.25	3.95	3.74	3.69	4.25	4.31	4.28	4.34
$u_*/(gSh)^{\frac{1}{2}}$	0.91	0.94	0.97	0.97	0.92	0.91	0.89	0.91	0.90	0.92
u_{\max} (cm/s)	75.7	77.7	85.9	79.3	83.3	84.9	95.8	98.8	100.4	100.4
$\langle \bar{u} \rangle^b$ (cm/s)	64.9	67.1	74.4	67.2	71.8	73.6	81.4	86.2	87.9	87.6
$\langle \langle \bar{u} \rangle \rangle^c$ (cm/s)	62.8	63.6	69.2	64.6	68.0	68.0	77.8	80.8	82.0	82.0
$c(\varphi = 0.1)$ ($\times 10^{-3}$) ^d	1.9	1.1	0.72	1.0	0.55	0.24	2.08	0.80	0.47	0.31
$c(\varphi = 0.1)$ ($\times 10^{-4}$)	0.94	0.31	0.05	0.21	0.22	0.13	0.65	0.42	0.29	0.19
d (mm)	0.15	0.19	0.24	0.19	0.19	0.19	0.19	0.19	0.19	0.19
σ_g	1.12	1.20	1.18	1.20	1.20	1.20	1.20	1.20	1.20	1.20
w_{s0} (cm/s)	1.6	2.3	3.1	2.3	2.3	2.3	2.3	2.3	2.3	2.3
w_{s0}/u_*	0.45	0.61	0.73	0.58	0.61	0.62	0.54	0.53	0.54	0.54
Fr $\equiv \langle \bar{u} \rangle / (gh)^{\frac{1}{2}}$	0.82	0.84	0.93	0.90	0.96	0.99	1.08	1.15	1.17	1.17
Re $_*$ $\equiv u_* h / \nu$ ($\times 10^3$)	2.31	2.44	2.78	2.26	2.13	2.10	2.34	2.28	2.30	2.30

^a Estimated using Reynolds-stress profiles (except 1565EQ).

^b Depth-averaged velocity, numerically integrated from centreline measurements.

^c Area-averaged velocity, based on bulk discharge and flow area.

^d Concentrations at $\varphi = 0.1$ and $\varphi = 0.5$ estimated from interpolation of measured concentration profiles.

TABLE 1. Summary of flow characteristics

comparative study, with clear-water results obtained under similar conditions and instrumentation as a standard, the necessity for any bias correction is debatable, provided the presence of sediment in suspension does not substantially affect sampling bias.

4.2. Experimental scope and constraints

The gross characteristics of the experiments performed are listed in table 1, each experiment being mnemonically labelled to indicate the nominal grain size, depth of flow and whether an equilibrium bed (EQ) or a starved bed (ST) exists. The study focused on equilibrium-bed flows since these offer a simplification in the context of similarity. A similarity approach with the associated scalings based on dimensional considerations, such as given in the preceding section, is most easily formulated where the number of relevant parameters is minimized. In the treatment of starved-bed or unsaturated flows, the degree of saturation adds a further parameter to be considered. Indeed, if multiple concentration scales are appropriate, it is not clear that the degree of saturation can be simply parametrized. The range of equilibrium-bed experiments feasible, given the flume geometry and the experimental technique, was constrained however by several factors. Flat equilibrium beds are achievable only in a narrow range of hydraulic and grain parameters, the limits of which are poorly understood. A parameter such as d cannot, in general, be independently varied, but requires a change in another parameter such as h , if a flat-bed condition is to be maintained. A constraint on h , due to aspect-ratio requirements, (aspect ratio

$b/h > 4$) may then impose an upper bound on d . On the other hand, a lower bound on d was dictated by the deterioration of the Doppler-signal quality with increasing suspended-sediment concentration. Only four experiments with flat equilibrium beds were therefore performed, with three very uniform (geometric standard deviation, $\sigma_g \approx 1.2$) natural sands. The thickness of the bed was typically ≈ 4 mm ($20\text{--}30d$). Starved-bed experiments, to which the proposed similarity model is not strictly applicable but which are not limited by the flat-bed constraints, were also performed in order to supplement the equilibrium-bed results over a wide range of conditions. These are labelled with an alphabetical suffix indicating the relative amount of sediment in suspension, with A being that with the heaviest suspended load. It is to be noted that total loads or depth-averaged concentrations are not given in table 1, these being notoriously difficult to measure or estimate accurately. Instead, the concentrations at two points, $\varphi = y/h = 0.1$ and 0.5 , estimated by interpolation from measurements, may be used as a guide to the level of suspension concentration. This characterization also accords with the emphasis on the two-scale nature of the concentration profile, which is hidden when only a depth-averaged concentration is given.

5. Experimental results

5.1. Results on Reynolds stress

Reliable two-component velocity measurements were obtained for all but one experiment, the exception being the equilibrium-bed experiment with the finest sand ($d = 0.15$ mm), the large suspended load precluding reliable measurements. Even so, such measurements were always limited to the region, $y/h > 0.1$, where the suspension was sufficiently dilute ($c < 10^{-3}$). Measured Reynolds stresses for equilibrium-bed and starved-bed experiments, normalized by the estimated wall-shear stress, are shown in figures 2 and 3. A tendency for the measured stresses to be less than the estimated linear profile in the region, $y/h > 0.5$, may be noted. This characteristic, also seen in preliminary clear-water experiments (Lyn 1986), is attributed to the greater importance of sidewall effects in the upper flow. In the case of 1565EQ, u_*^2 was estimated as $u_*^2 = A gSh$, where A is a proportionality factor, chosen to be 0.91 on the basis of the values of u_*^2/gSh obtained in the other experiments.

5.2. Velocity-defect profiles

Velocity-defect profiles for the equilibrium-bed experiments are compared in figure 4 with fits according to the traditional practice and to the more recent suggestion of Coleman (1981). κ_s is seen to be less than 0.4, and, if attention is confined to those experiments of the same depth, $h = 6.5$ cm, decreases with decreasing sand size (and hence increasing suspended load). Such features agree qualitatively with traditional expectations. Nevertheless, closer examination reveals that, while the traditional approach may provide an overall fit, it does not track the experimental points in detail. In the model of Coleman, deviations in the region $y/h < 0.1$ are more marked, although the fit is marginally better than the traditional in the outer region; to some extent, this may be due to the particular fitting algorithm used which tends to give more weight to deviations in the outer flow. Nevertheless, in all cases, the slope of the profile in the inner region is definitely larger than that associated with a value of $\kappa_s \approx 0.4$, contrary to recent assertions. Further, the values of W_0 obtained from the fit do not differ significantly from those found in clear-water experiments, where $W_0 \approx 0.2$ (Lyn 1986; Nezu & Rodi 1986).

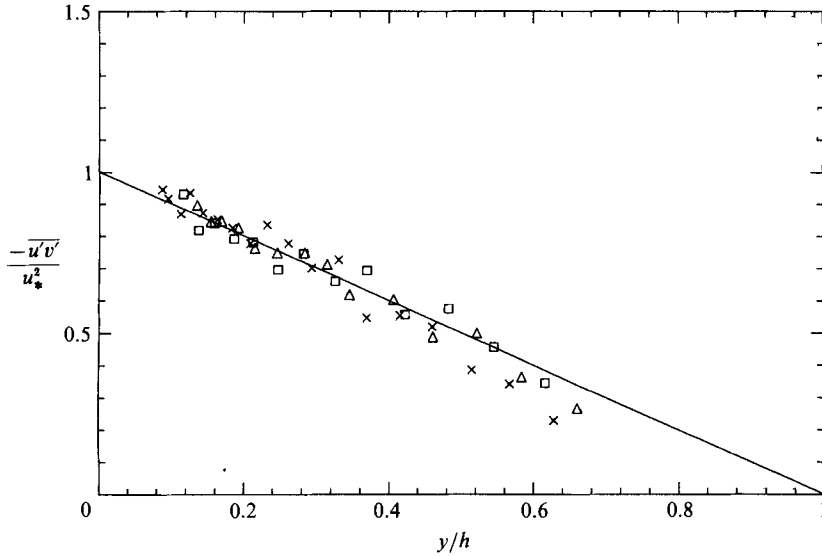


FIGURE 2. Reynolds stress profiles for equilibrium-bed experiments (in this and the following plots, symbols are as given in table 1 unless otherwise indicated).

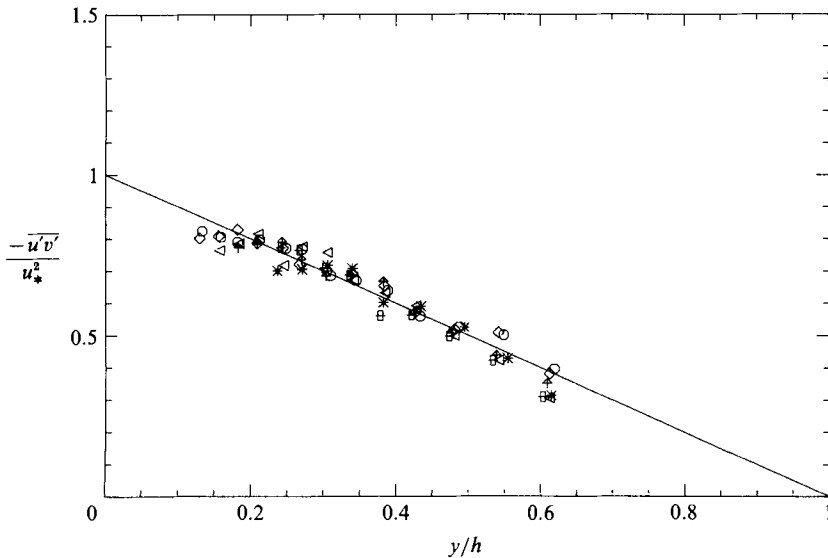


FIGURE 3. Reynolds stress profiles for starved-bed experiments.

The velocity-defect profiles for all equilibrium-bed experiments are plotted in figure 5, but interpretation is made difficult by the scatter in the upper region of flow. This scatter is largely due to variations in y_{\max}/h (also to be found in the preliminary clear-water experiments). A clearer picture is found in figure 6, which shows the results of only two of the equilibrium-bed experiments, and a clear-water experiment, all with approximately the same $y_{\max}/h \approx 0.81$. A solid line representing what may be considered a model clear-water profile, obtained from (2.2) with $W_0 = 0.2$, is also plotted. The effect of sediment is found only in the lower region of flow; the sediment-laden flow profiles essentially coincide with the clear-water flow profile

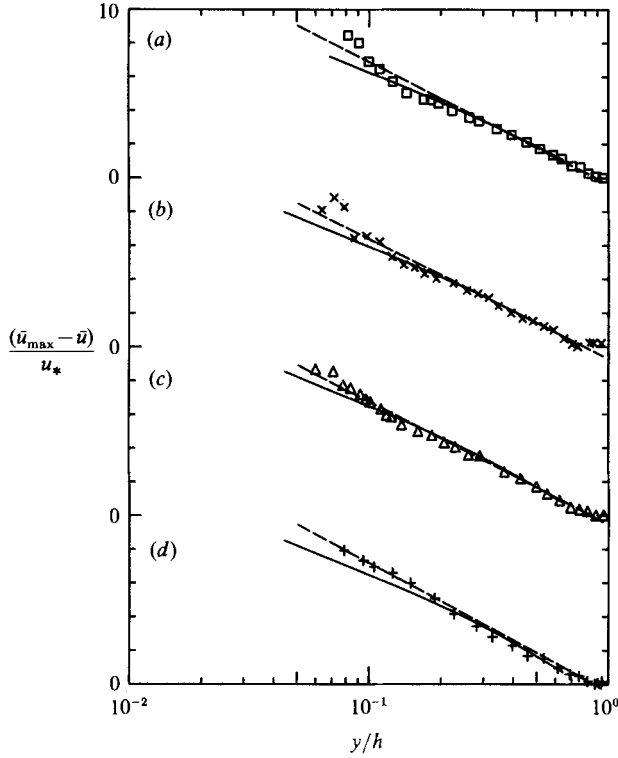


FIGURE 4. Comparison of equilibrium-bed velocity-defect profiles with fits according to the Coleman model (—, variable W_0) and the traditional model (---, variable κ_s), (a) 1957EQ, $\kappa_s = 0.316$; $y_{\max}/h = 0.93$, $W_0 = 0.14$; (b) 2565EQ, $\kappa_s = 0.32$; $y_{\max}/h = 0.81$; (c) 1965EQ, $\kappa_s = 0.32$; $y_{\max}/h = 0.81$, $W_0 = 0.25$; (d) 1565EQ, $\kappa_s = 0.30$; $y_{\max}/h = 0.81$, $W_0 = 0.26$.

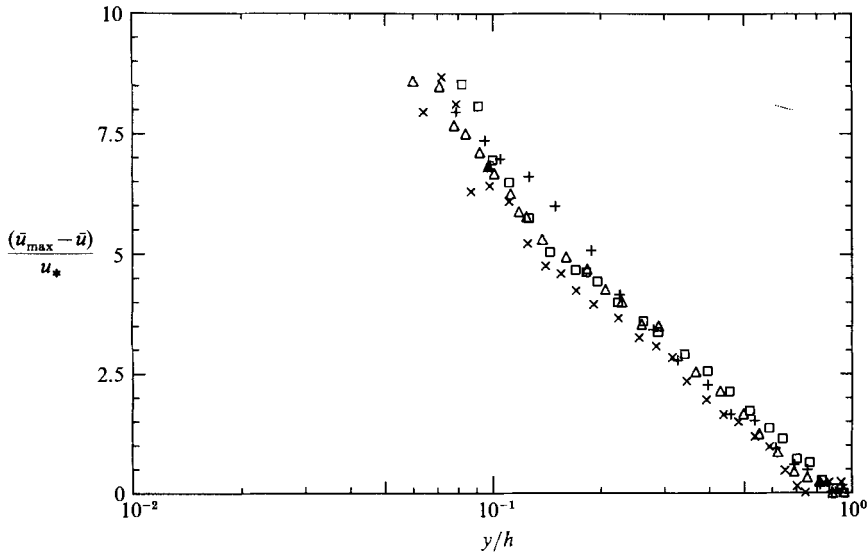


FIGURE 5. Velocity-defect profiles for all equilibrium-bed experiments.

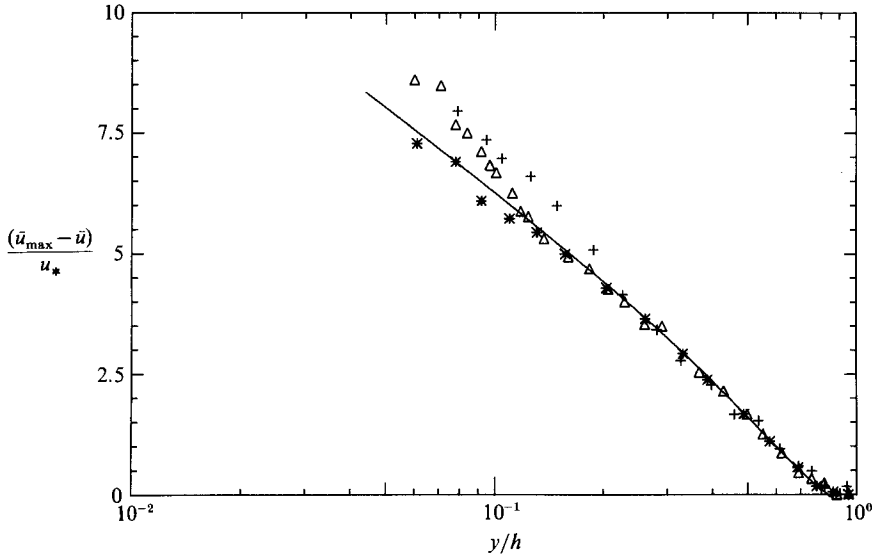


FIGURE 6. Comparison of velocity-defect profiles for equilibrium-bed experiments, 1965EQ and 1565EQ, and a clear-water experiment, *, (Lyn 1986), and model clear-water profile with $W_0 = 0.2$ in equation (2.2).

for $y/h > 0.25$. These profiles also suggest the trend that, as the local sediment concentration increases from 1965EQ to 1565EQ, the region of a marked deviation from the clear-water profile extends upwards into the bulk of the flow. In the case of 1965EQ, the deviation is confined to a relatively small region, $y/h < 0.1$, and, consequently, an intermediate region can be clearly discerned that is distinct from either the 'wake' region or the region affected by the sediment. Since the profile from 1965EQ coincides with the clear-water profile in this region, it approaches an approximately logarithmic profile with an associated $\kappa_s = \kappa \approx 0.4$. In the case of 1565EQ, where region of deviation is more extensive, the distinction from the wake region becomes more tenuous, and the existence of a definite log region may be debated.

The same qualitative behaviour is also observed in the velocity-defect profiles from two series of starved-bed experiments (figures 7 and 8), in which u_* , h , d and w_{s0} , were kept constant, and only the suspended load was changed by adding sediment to the flow. In the lower-transport series, 1957ST-1, the central part of the channel was free of any visible permanent deposition, but ripples oblique to the flow were formed at both corners of the flume and extended about 5 cm into the flow. During the higher-transport series, 1957ST-2, the flume was entirely free of any permanent noticeable deposition. In figure 7 especially, the profiles from the two starved-bed experiments and the equilibrium-bed experiment coincide with the model clear-water profile (here W_0 was taken to be 0.15) for $y/h > 0.15$. An intermediate region that approaches the clear-water logarithmic profile can be clearly discerned, and the magnitude of the deviation from the clear-water profile increases with increasing suspended load. In the higher-transport series, the trend to a more extensive affected region with increasing suspended load is also seen, the distinction between the outer region and the region affected by the sediment being already blurred in the case with the heaviest suspended load, 1957ST-2:A. These starved-bed results eliminate the possibility of explaining the equilibrium-bed results in terms of phenomena requiring the existence of an actual sand bed rather than of a simple suspension.

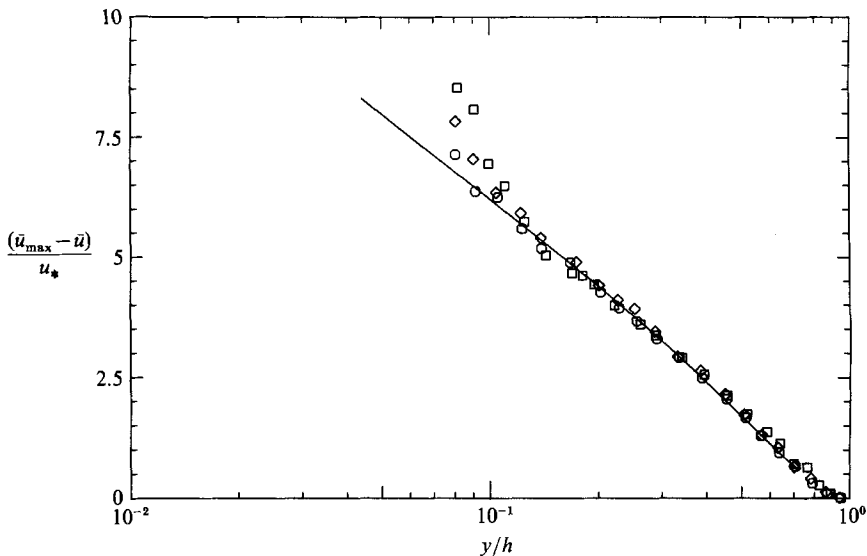


FIGURE 7. Comparison of starved-bed and model clear-water profiles: series 1957ST-1.

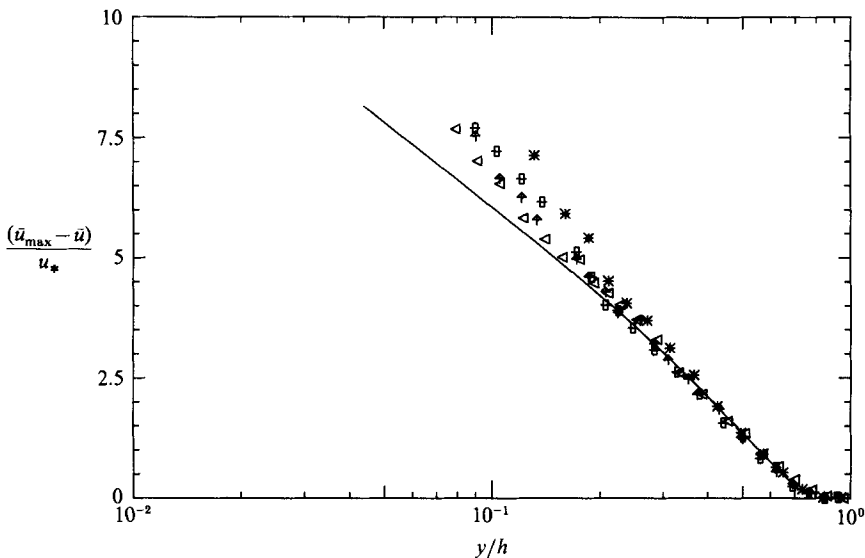


FIGURE 8. Comparison of starved-bed and model clear-water profiles: series 1957ST-2.

These experimental results conflict qualitatively with both the traditional model and the more recent stratified-flow models. Rather than the global effect implied by the former, a largely local effect is seen to be possible. On the other hand, the localized effect in the outer region expected by the latter is not observed, but rather a localized effect in the inner region is found. The somewhat limited range of conditions spanned by the present study should be emphasized; there are some indications that other conditions, e.g. a heavier suspended load, may result in a more global effect, and there may be a range of conditions where the effect is localized in the outer flow. A need would remain to explain or at least characterize the present results.

The question arises whether these effects may be attributed entirely to the use of the LDV technique, since the sediment concentration is highest near the bottom, with a consequent increase in the difficulty of measurements. Even if such were the case, however, the results in the upper region, $y/h > 0.2$, where the reliability of measurements is much higher, would still not support previous theories proposed for sediment concentrations of comparable magnitude. If the lower-region results are disregarded, then it can at most be concluded that there is little evidence to support the claim that the presence of sediment substantially affects the velocity profile. Further, if the trend already noted to a more extensive affected region with higher sediment concentrations is extrapolated, then the present results would be qualitatively consistent with some previous experimental results, since a larger velocity defect than that in clear-water flow would be found throughout the depth. While previous theories described this in terms of a small κ_s or a larger wake coefficient, W_0 , the present view emphasizes its relation to a more localized phenomena that is found to occur at smaller concentrations. Finally, the experiment, 1565EQ, was designed to duplicate in essential respects an experiment of Brooks (1954) (run 7), by using the same sand and the same channel; the depth of flow was reduced from 7.4 cm to 6.5 cm to satisfy the aspect-ratio constraint, and the estimates of wall shear differ slightly. Brooks' results, obtained by the traditional Pitot-tube method, were found (Lyn 1986) to compare quantitatively well with the present results. These tend to support the conclusion that the LDV technique is as reliable qualitatively and quantitatively as traditional techniques, and further that the results are not inconsistent with previous experimental results, although their interpretation may differ.

5.3. Concentration profiles

In figures 9 and 10 are presented the concentration profiles of equilibrium-bed experiments and in the starved-bed experiment with the heaviest suspended load, 1957ST-2:A. Two possible scaling are examined: one in which y is scaled by h , an outer scale, and another by $u_*^2/g(s-1)$, a scale associated with a stratified-flow analogy. Neither is satisfactory in illuminating the results. Discussion of concentration profiles is more complicated than velocity profiles because (i) there is no equivalent to the clear-water velocity profile which may be used as a standard for comparison, and (ii) a generally accepted scaling such as the velocity-defect law is not available. Some qualitative characteristics, usually taken for granted but which gain in significance in the context of a multiple-scales similarity theory, may be noted. The orders-of-magnitude variation in local concentration clearly differs from that seen in the velocity profile, and rules out any logarithmic profile, and also suggest the inadequacy of a single common concentration scale. From these log-log plots, it seems unlikely that any simple power-law with a constant exponent describes all of these profiles, even in some finite intermediate region. Even if an appropriate concentration scale could be defined, this could only shift the curves up or down and would not change their slopes.

5.4. The perspective of the proposed similarity model

The proposed similarity model hypothesized a local effect in the inner region, implying the existence of an inner lengthscale whose scaling must be determined. In figures 11 and 12, the equilibrium-bed profiles are plotted in inner coordinates based on viscous and on roughness (or grain-size) scaling. The large scatter resulting from either scaling strongly suggests that neither is appropriate. Further evidence is found in particular examples. Both 2565EQ and 1957ST-2:A were performed at the same

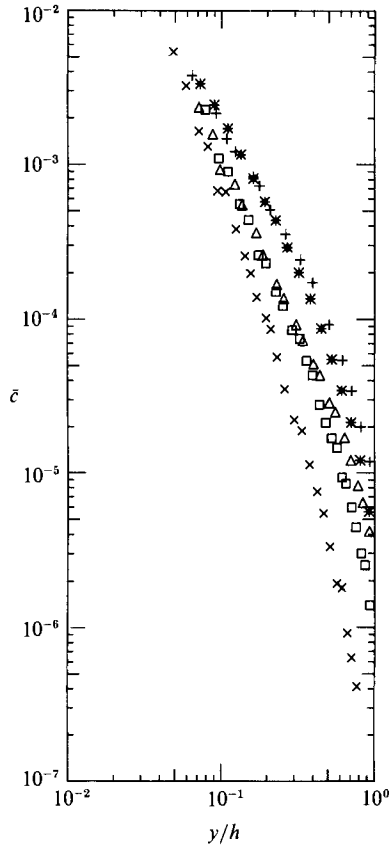


FIGURE 9. Mean concentration profiles, plotted in outer coordinates, \bar{c} vs. y/h .

u_* and thus l_v is the same in both cases; their velocity profiles, however, differ significantly in that an approximately logarithmic region may be clearly seen in 2565EQ, but has practically disappeared in 1957ST-2:A. Similarly, 1957EQ and 1957ST-2:A were performed with the same sand, such that d is the same, but the resulting profiles are seen to be quite different. Although 1957ST-2:A is not strictly an equilibrium-bed experiment and so may not be strictly comparable, the results in figures 7 and 8 indicate that increasing sediment concentration in starved-bed experiments leads to a more extensive effect on the velocity-defect profile. If an equilibrium-bed had been achieved under the same conditions as were obtained in the starved-bed series, 1957ST-2, it is expected that the conclusions would indeed be reinforced.

In figure 11, a significant downwards shift of the velocity profile in sediment-laden flows in comparison to a clear-water flow may be noted. In addition, therefore, to the effect emphasized in the preceding section, of a deviation from the clear-water velocity-defect profile in the inner region, this additional effect, much like that of an increased roughness, is also typically observed. Some of this increased roughness in the equilibrium-bed flow results may be attributed to the bed not being perfectly flat. Since the same effect can also be found in starved-bed flows (Lyn 1986), it is clear that not all of this increase can be so explained and that some of this must be due to the sediment in suspension. Further, that this displacement is already apparent in the inner flow suggests that it is primarily due to the higher concentration near-bed

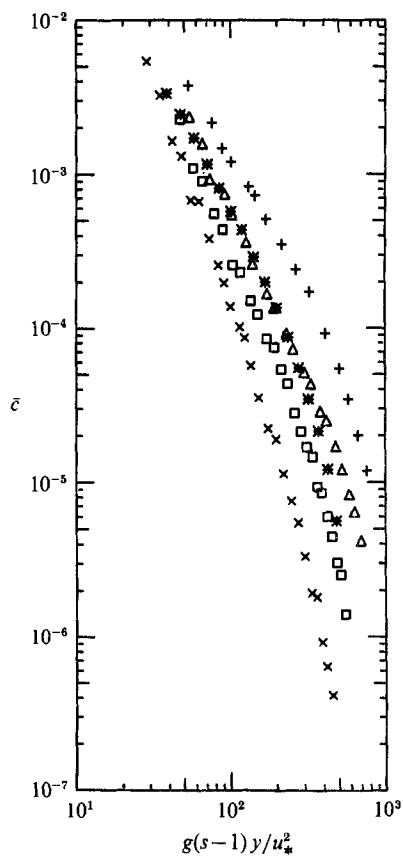


FIGURE 10. Mean concentration profiles, plotted in coordinates suggested by the stratified-flow analogy, \bar{c} vs. $g(s-1)y/u_*^2$.

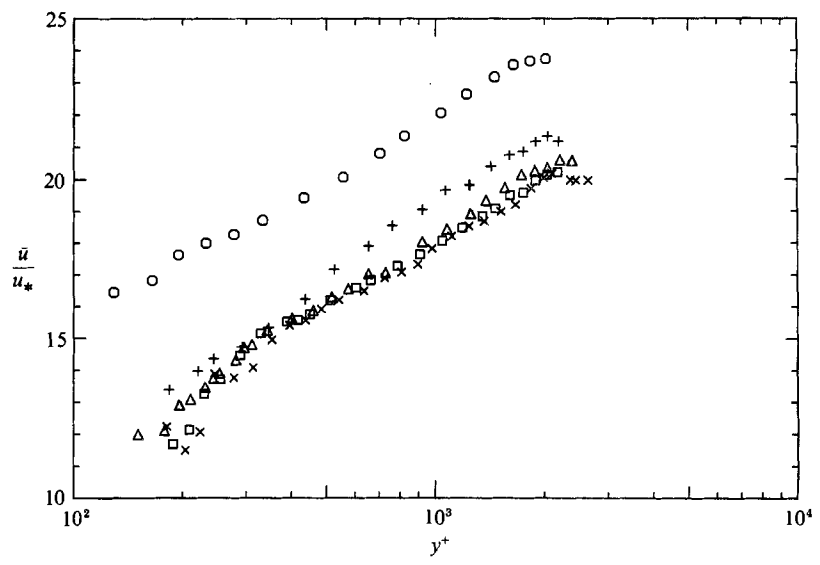


FIGURE 11. Comparison of equilibrium-bed velocity profiles with a clear-water profile, ○, (Lyn 1986) in viscous coordinates, \bar{u}/u_* vs. $y/(\nu/u_*)$.

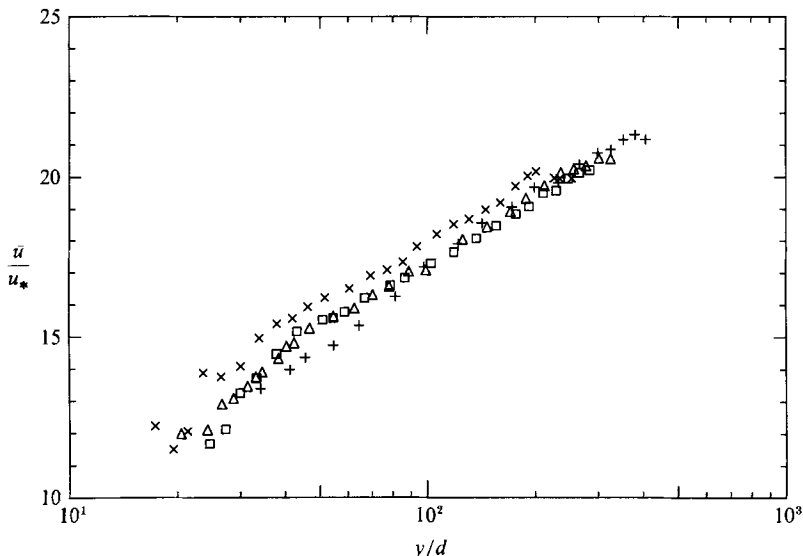


FIGURE 12. Equilibrium-bed velocity profiles in roughness coordinates, \bar{u}/u_* vs. y/d .

sediment rather than the bulk suspended sediment. Although of some practical importance since it implies a larger friction factor than in clear-water flows, if such a shift were the only manifestation of the presence of suspended sediment, then the problem would be somewhat less interesting since the total effect of the sediment could arguably be modelled as an effective roughness.

The proposed inner scale, l_s , depends in a complicated way on hydraulic and grain parameters involving an unknown function of at least w_{s0}/u_* (3.9) and possibly also $g(s-1)d/w_{s0}^2$ (3.8). If a distinct inner layer and the corresponding log layer can be distinguished, then an appropriate choice of a reference velocity, u_s , and of l_s , will collapse the velocity profiles in the log layer on to a line defined by

$$\frac{\bar{u}_s - \bar{u}}{u_*} = -\frac{1}{\kappa} \ln \xi_s, \quad (5.1)$$

where $\xi_s = y/l_s$, and any additive constant has been absorbed into \bar{u}_s . This process is essentially equivalent to defining l_s as the point where the velocity profile deviates from the log law in the inner region. This is not the most desirable definition; were the viscous scale to be similarly defined, then it would be $\approx 50\nu/u_*$, i.e. far larger than would be conventionally considered. For qualitative comparisons, however, it should be sufficient.

By a trial-and-error procedure, \bar{u}_s and l_s were chosen to obtain a good collapse of the data. The values of \bar{u}_s and l_s , as well as dimensionless ratios involving l_s are given in table 2. The results are plotted in figure 13. In cases where an extensive log-like region exists, i.e. all except possibly 1565EQ and 1957ST-2:A, the collapse of the data in this region may be considered quite good. The inner scale, l_s , so obtained is plotted in its non-dimensional form, $\Delta_s = g(s-1)l_s/u_*^2$, against w_{s0}/u_* , in figure 14. In the range of w_{s0}/u_* examined, Δ_s is seen to be sensitive to changes in w_{s0}/u_* , decreasing like $(w_{s0}/u_*)^{-n}$, where $2 < n < 3$. The inclusion of the point from 1957ST-2:A is an approximation, since it is not obtained from an equilibrium-bed experiment in which case it would probably give a somewhat larger Δ_s . To the extent

Run	l_s (cm)	l_s/h	l_s/d_{50}	l_s/l_v	u_s (cm/s)
1565EQ	1.3	0.20	87	468	60
1965EQ	0.6	0.09	32	225	54
2565EQ	0.5	0.08	22	223	59
1957EQ	0.6	0.11	33	249	57
1957ST-2:A	1.3	0.22	68	553	79

TABLE 2. Parameter values used in collapsing velocity profiles

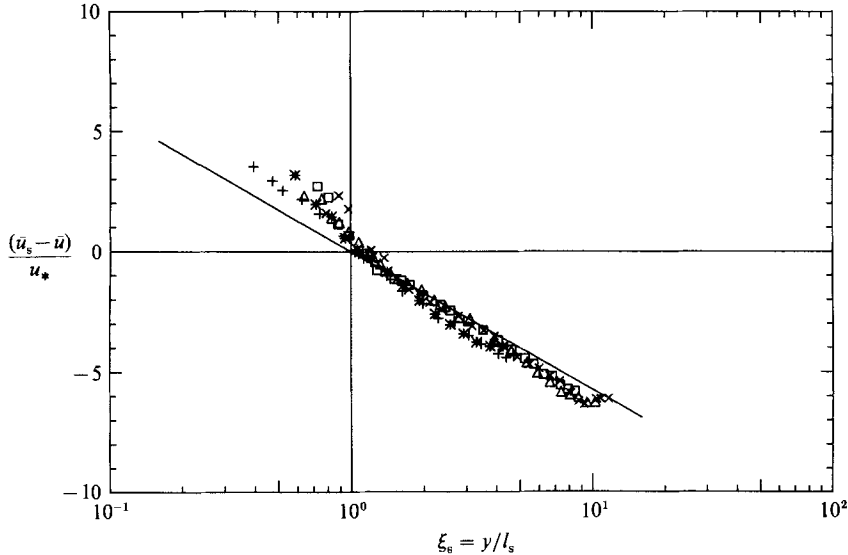


FIGURE 13. Velocity-defect profiles in proposed similarity coordinates.

that Δ_s seems to correlate well with w_{s0}/u_* alone, the effect of the grain diameter seems to be negligible, such that the simplified relation (3.9) seems to be an adequate approximation to the more complete expression (3.8).

With l_s determined from the analysis of the velocity profile, the concentration profile can be treated in an analogous manner, where the exponent Z is analogous to u_* in its role of scaling not the concentration but rather the log of the concentration. This exponent and a concentration scale, c_s , were found by requiring that the concentration profiles in the region, $\xi_s \gg 1$, $y/h \ll 1$, (interpreted here rather loosely), collapse onto a line defined by

$$\frac{\log \bar{c} - \log c_s}{Z} = -\log \xi_s. \quad (5.2)$$

as shown in figure 15. The deviation from the -1 power line (on this plot) as the free surface is approached is clear, and is reminiscent of an analogous deviation in the velocity profile, thereby motivating a 'wake' treatment of the concentration profile also (Lyn 1986). The proposed similarity theory suggests that the concentration profile like the velocity profile, would also deviate from the asymptotic law of the overlap region in $\xi_s \ll 1$ (as well as in $y/h = O(1)$). The results of figure 15 do not exhibit any marked deviation of $\xi_s < 1$, although a tendency for the magnitudes to be slightly larger than that associated with the -1 power line may be discerned.

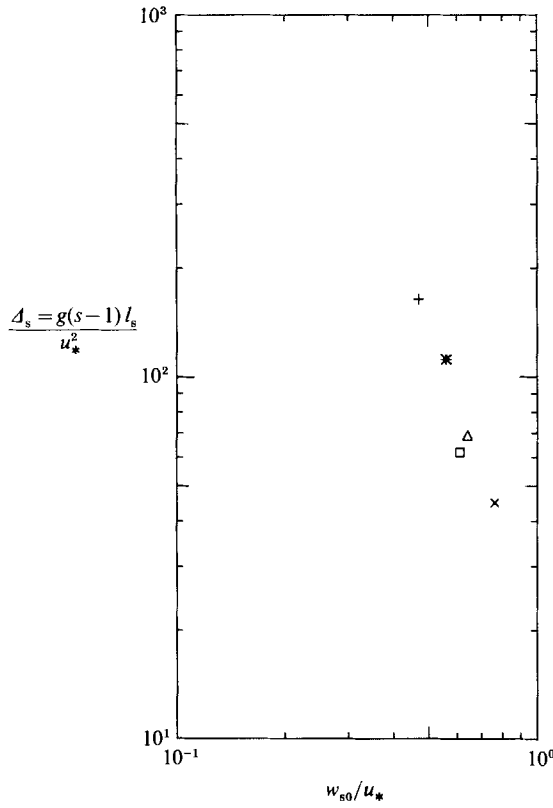


FIGURE 14. The non-dimensional inner lengthscale, Δ_s , as a function of w_{s0}/u_* .

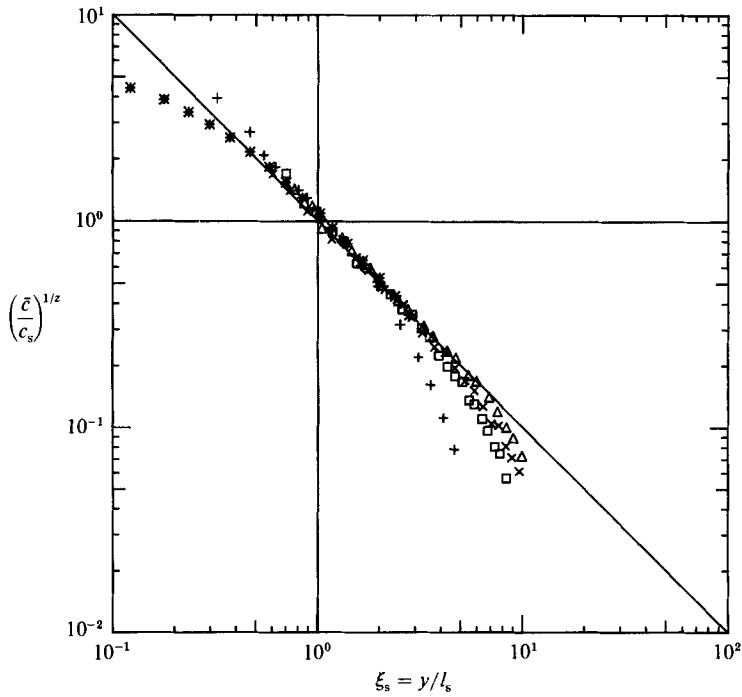


FIGURE 15. Mean concentration profiles in proposed similarity coordinates.

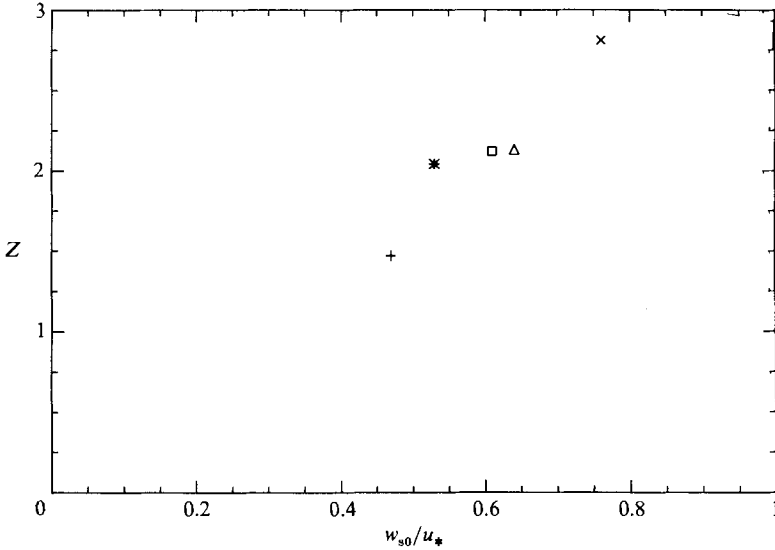


FIGURE 16. The power-law exponent, Z , as a function of w_{s0}/u_* .

Some evidence of such a deviation can be found in some previous experimental results of Barton & Lin (1955), but these are perhaps too limited to support a definitive conclusion. (Previous data regarding the velocity as well as the concentration profile are discussed at length in Lyn 1986.) The exceptional case of 1957ST-2:A is again attributed to the non-equilibrium nature of the experiment.

The corresponding values of Z are plotted in figure 16 against w_{s0}/u_* . A simple version of the mixing-length model along traditional lines assumes that $\beta_s \kappa_s$ is constant, thus predicting a linear variation of Z (or more precisely Z_R) with w_{s0}/u_* (or w_s/u_*), with $Z \rightarrow 0$ as $w_{s0}/u_* \rightarrow 0$. If the result for 1957ST-2:A is ignored, then the dependence of Z on w_{s0}/u_* is well approximated by a linear function, which, however, does not vanish as $w_{s0}/u_* \rightarrow 0$. It is speculated that the value of Z for 1957ST-2:A would decrease under the equivalent equilibrium-bed conditions and so would agree more with the other results. Inclusions of the point from 1957ST-2:A as is, and requiring that $Z \rightarrow 0$ would give noticeably greater scatter. The weakness and the strength of the similarity approach is that it does not make any claims concerning the nature of the variation of Z with w_{s0}/u_* . On the other hand, the traditional result has little practical advantage if, as seems likely, $\beta_s \kappa_s$ is not constant, even though it gives a superficially more precise result. The similarity model does make the further statement regarding the traditional result that, if $\beta_s \kappa_s$ is not constant, then it depends only on w_{s0}/u_* (assuming that $w_s/u_* \approx w_{s0}/u_*$). A plot of the concentration scale, c_s , against w_{s0}/u_* is shown in figure 17. Since $c_s \approx c(\xi_s)$, its variation largely reflects the magnitude of l_s ; a larger l_s as in 1565EQ and 1957ST-2:A is associated with a smaller c_s . This information may also be expressed in an alternative form in terms of the function, $\mathcal{E}_s(w_{s0}/u_*) = g(s-1) c_s^{1/Z} l_s / u_*^2 = c_s^{1/Z} \Delta_s$, which is plotted in figure 18. The special behaviour of the point from 1957ST-2:A is again attributed to the non-equilibrium nature, to which c_s , l_s , and particularly Z may be sensitive.

An inner lengthscale differing from either the viscous or the roughness scale is conceptually consistent with the experimental results, particularly in the case of the velocity profile. A physical interpretation, more detailed than that involved in the

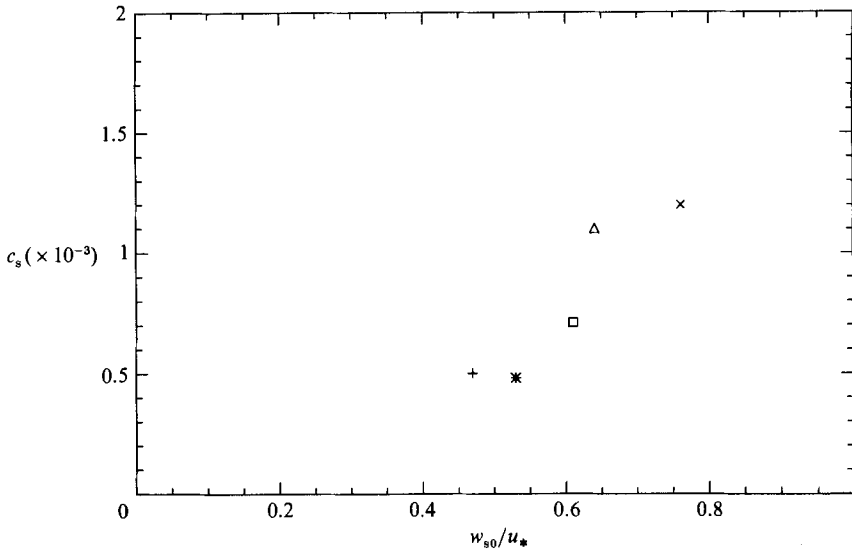


FIGURE 17. The concentration scale, c_s , as a function of w_{s0}/u_* .

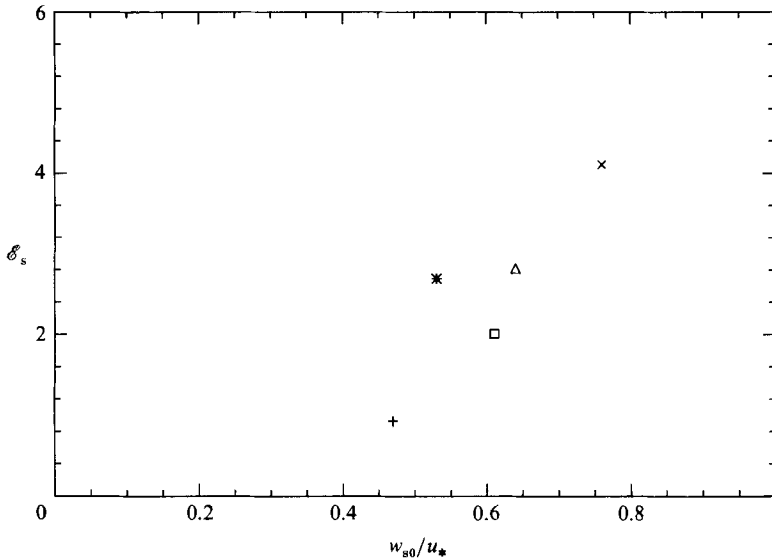


FIGURE 18. The multiplicative parameter, E_s , (equation (3.16)) as a function of w_{s0}/u_* .

formal dimensional reasoning of §3, is rather speculative at this time, but the fact that the sediment concentration is largest near the bed perhaps gives a clue. The special character of the near-bed concentration doubtless played a role in the definition of Ri_C by Coleman (1981) and, before that, in the modification of the Einstein–Chien parameter by Vanoni & Nomicos (1960). As the bed is approached, smaller, higher-frequency scales, and consequently particle-fluid slip, gain in importance. The retarded near-bed velocities, reminiscent of roughness effects, may then be a reflection of the ensemble effect of this slip. At the same time, the slower, larger scales which dominate the outer flow are only negligibly, if at all, affected by the particles. The localized nature is further reinforced by the large gradients in concentration near the bed, such that the region of high sediment concentration may

be relatively thin. Unlike simple roughness effects, however, the sediment effects may have a significantly larger range of influence, perhaps even extending throughout the flow under special conditions, and depends not on a single parameter like the roughness height, but rather on a combination of hydraulic and grain parameters. Thus, a relatively undisturbed outer flow and a retarded inner flow combine to give a velocity profile, with gradient in some regions larger than those found in clear-water flows. If, as in most of the present results, the inner flow region is sufficiently small, then a definite log region, with $\kappa \approx 0.4$, may be discerned, the larger gradient region being found below the log region.

While the necessity for an inner lengthscale is evident in the analysis of the velocity profile, it is more debatable in the analysis of the concentration profile. To some extent, this may be due to the methodological difficulties noted in §5.3. It is possible that the concentration profile is characterized by its own inner scale, independent of and much smaller than the inner scale of the velocity profile so as to be unobservable in the present experimental results. This possibility is less attractive in turbulent flows than in laminar flows, and would certainly make for a more involved theory. Even if such were the case, this would still fit within a similarity framework, with changes only in the choice of scales. This may also be the case when the effect of the sediment is more global.

6. Summary and conclusions

A conceptual framework for treating the coupled mean fields in sediment-laden open-channel flows has been developed. Rather than being based on eddy-diffusivity models or a Reynolds analogy as in past models, it makes general hypotheses regarding similarity, multiple scales, and asymptotic matching. Asymptotic power laws with varying exponent, applicable to the concentration profile, are shown to be associated with disparate concentration scales in the inner and outer flow regions and a dimensionless parameter important in both regions. This contrasts with the velocity field, which is characterized by a single common velocity scale, for which an asymptotic logarithmic profile is more appropriate. The analysis clarifies some of the implicit assumptions of previous models, and provides for a more flexible approach. The need for this flexibility is shown in the experimental results for the velocity profile, where it was seen that, for a range of laboratory conditions, the effect of sediment was confined to a layer adjacent to the bed. An intermediate region could be discerned in which the velocity and the concentration profiles may be approximately described by asymptotic log-law ($\kappa_s = \kappa \approx 0.4$) and power-law profiles (with exponent varying with w_{s0}/u_* only) respectively. The suggested length and concentration scales are however complicated in that they involve an unknown function of w_{s0}/u_* which must be determined empirically. The proposed model does not preclude the possibility of cases in which the effect of sediment extends throughout the flow; the experimental results indicate that this may arise with heavy suspended loads. In such cases, the basic similarity framework may still be valid with modifications only in the choice of scales.

The work reported here is largely based on the author's Ph.D. dissertation under the supervision of Professor N. H. Brooks at the W. M. Keck Laboratory of Hydraulics and Water Resources, California Institute of Technology, Pasadena, and was financially supported by the National Science Foundation (Grants CEE-7920311 and

MSM-8611127) and the James Irvine Professorship. The author also acknowledges personal support in the form of a Haagen-Smit/Tyler Fellowship and fellowships from the National Science and Engineering Research Council of Canada.

Appendix: A matching argument

The following extends the argument found in Tennekes & Lumley (1980). It is assumed that, in a given flow region, only two lengthscales, l and \mathcal{L} , are of possible importance, with $\mathcal{L}/l \gg 1$. Two regions are distinguished: the inner region, $y/l = O(1)$, $y/\mathcal{L} \ll 1$, and the outer region, $y/l \gg 1$, $y/\mathcal{L} = O(1)$. A general inner law for a dependent variable, r , may be expressed formally as

$$\left(\frac{r}{r_*}\right)_i = f\left(\frac{y}{l}, \frac{y}{\mathcal{L}}\right), \tag{A 1}$$

where r_* is an appropriate scale for r . An outer law may be similarly expressed as

$$\left(\frac{r}{r_*}\right)_o = F\left(\frac{y}{l}, \frac{y}{\mathcal{L}}\right). \tag{A 2}$$

The scale, r_* , is assumed to be common to both regions (much as u_* scales both inner and outer laws in the conventional argument for the velocity profile). The variables, $\xi = y/l$ and $\varphi = y/\mathcal{L}$, are then treated as essentially independent in the asymptotic limit, $\mathcal{L}/l \rightarrow \infty$. The gradient of r is assumed to match in an intermediate overlap region, $\xi \rightarrow \infty$, $\varphi \rightarrow 0$, such that, after multiplication by y ,

$$\xi \frac{\partial f}{\partial \xi} + \varphi \frac{\partial f}{\partial \varphi} = \xi \frac{\partial F}{\partial \xi} + \varphi \frac{\partial F}{\partial \varphi}. \tag{A 3}$$

The desired solution is found where both f and F are such that the operation, $\mathcal{T}\Phi$, where $\mathcal{T} \equiv \xi\partial/\partial\xi + \varphi\partial/\partial\varphi$, and Φ is either f or F , results in the possibility of a separation of variables. A particular class of functions is that where f (or F) is itself separable; i.e.

$$f = f_1(\xi)f_2(\varphi). \tag{A 4}$$

For this class of functions, the separability condition is found to be

$$\varphi f'_2(\varphi) = \lambda_1 f_2(\varphi), \tag{A 5}$$

with λ_1 as an undetermined constant (a similar relation with f_1 is also found). This suggests that a more useful form of similarity laws than either (A 1) or (A 2) may be expressed as

$$\left(\frac{r}{r_*}\right)_i = \varphi^{\lambda_1} \Phi_1(\xi), \tag{A 6}$$

$$\left(\frac{r}{r_*}\right)_o = \xi^{\lambda_2} \Phi_2(\varphi). \tag{A 7}$$

The form of (A 6) and (A 7) was chosen in order that the special degenerate case treated by the conventional argument is included when $\lambda_1 = \lambda_2 = 0$ (and a defect law is used instead of (A 7)). Substitution of (A 6) and (A 7) into (A 3) reveals that, for $\lambda_1 \neq 0$ and $\lambda_2 \neq 0$, r varies in the overlap region as

$$\frac{r}{r_\xi} = C_1 \xi^\lambda + C_{21}. \tag{A 8}$$

where a new inner scale is defined as $r_\xi \equiv r_*(l/\mathcal{L})^{\lambda_1}$, $\lambda = \lambda_1 + \lambda_2$, and C_1 and C_{21} are integration constants. A similar result in outer coordinates is also found with a new outer scale $r_\varphi \equiv r_*(l/\mathcal{L})^{-\lambda_2}$, a new additive constant, C_{20} , but the same multiplicative constant, C_1 . The form of (A 8) differs from the log law in that, rather than a common unique scale as first assumed for both the inner and outer regions, two scales are found to be necessary, namely, r_ξ and r_φ . Since

$$\frac{r_\xi}{r_\varphi} = \left(\frac{l}{\mathcal{L}}\right)^\lambda, \quad (\text{A } 9)$$

and $l/\mathcal{L} \ll 1$, these must be disparate scales unless $\lambda = 0$. The classic log law is seen to be a special degenerate case in which there is a common unique scale for the dependent variable for both inner and outer regions. It is, however, imbedded in a much wider class of profiles which multiple scales for both dependent and independent variables allow.

REFERENCES

- BARENBLATT, G. I. 1953 *Prikl. Math. Mech.* **16**, 67–78.
- BARENBLATT, G. I. 1979 *Similarity, Self-Similarity, and Intermediate Asymptotics* (translated from the Russian). New York: Consultants Bureau.
- BARTON, J. R. & LIN, P.-N. 1955 A study of the sediment transport in alluvial streams. *Civil Engineering Dept Rep. Colorado A & M College, Fort Collins*.
- BATCHELOR, G. K. 1965 *Proc. of the 2nd Australasian Conf. on Hydraulics and Fluid Mech.* O19–O41.
- BROOKS, N. H. 1954 Laboratory studies of the mechanics of motion of streams flowing over a moveable-bed of fine sand. Ph.D. thesis, California Inst. of Tech., Pasadena.
- COLEMAN, N. L. 1981 *J. Hydraul. Res.* **19**, 211–229.
- COLES, D. 1971 *Proc. AFOSR-IFP Stanford Conf. on Computation of Turbulent Boundary Layers 1968* (ed. D. Coles & E. Hirst), vol. 2, pp. 1–48. Stanford University California.
- EINSTEIN, H. A. & CHIEN, N. 1955 Effects of heavy sediment concentration near the Bedon velocity and sediment distribution. *MRD series 8*. University of California, Institute of Engineering Research and United States Army Engineering Division, Missouri River, Corps of Engineers, Omaha, Nebraska.
- HINO, H. 1963 *J. Hydraul. Div. ASCE*, HY4, 161–185.
- ITAKURA, T. & KISHI, T. 1980 *J. Hydraulics Div. ASCE*, HY 8, 1325–1343.
- IZAKSON, A. 1937 *Zh. Eksper. Teor. Fiz.* **7**, no. 7.
- LUMLEY, J. L. 1976 Two-phase and non-Newtonian flows, in *Turbulence* (ed. P. Bradshaw), pp. 289–324. Springer.
- LYN, D. A. 1986 Turbulence and turbulent transport in sediment-laden open-channel flows. Ph.D. thesis, California Inst. of Tech., Pasadena.
- MILLIKAN, C. B. 1939 *Proc. of the 5th Int. Congr. Appl. Mech.* pp. 386–392. Cambridge, MA.
- MONIN, A. S. & YAGLOM, A. M. 1971 *Statistical Fluid Mechanics*, vol. 1. Cambridge, MA: MIT Press.
- NEZU, I. & RODI, W. 1986 *J. Hydraul. Engng* **112**, 335–355.
- VAN RIJN, L. C. 1984 *J. Hydraul. Engng* **110**, 1613–1641.
- SAFFMAN, P. G. 1962 *J. Fluid Mech.* **13**, 120–128.
- SHEPPARD, P. A. 1946 *Proc. R. Soc. Lond.* A**118**, 208.
- TENNEKES, H. & LUMLEY, J. L. 1980 *A First Course in Turbulence*. Cambridge, MA: MIT Press.
- VANONI, V. A. 1946 *Trans. ASCE* **111**, paper no. 2267, 67–133.
- VANONI, V. A. & NOMICOS, G. N. 1960 *Trans. ASCE* **125**, paper no. 3055, 1140–1175.